Third AO4ELT Conference - Adaptive Optics for Extremely Large Telescopes
Florence, Italy. May 2013
ISBN: 978-88-908876-0-4
DOI: 10.12839/AO4ELT3.13358

POINT SPREAD FUNCTION EXTRACTION IN CROWDED FIELDS USING BLIND DECONVOLUTION

Laura Schreiber[1a], Andrea La Camera[2b], Marco Prato[3c], and Emiliano Diolaiti[1]

[1] INAF - Osservatorio Astronomico di Bologna, Via Ranzani 1, 40127 Bologna, Italia
[2] Dipartimento di Informatica, Bioingegneria, Robotica e Ingegneria dei Sistemi (Università di Genova), Via Dodecaneso 35, 16145 Genova, Italia
[3] Dipartimento di Scienze Fisiche, Informatiche e Matematiche (Università di Modena e Reggio Emilia), Via Campi 213/b, 41125 Modena, Italia

Abstract. The extraction of the Point Spread Function (PSF) from astronomical data is an important issue for data reduction packages for stellar photometry that use PSF fitting. High resolution Adaptive Optics images are characterized by a highly structured PSF that cannot be represented by any simple analytical model. Even a numerical PSF extracted from the frame can be affected by the field crowding effects. In this paper we use blind deconvolution in order to find an approximation of both the unknown object and the unknown PSF. In particular we adopt an iterative inexact alternating minimization method where each iteration (that we call outer iteration) consists in alternating an update of the object and of the PSF by means of fixed numbers of (inner) iterations of the Scaled Gradient Projection (SGP) method. The use of SGP allows the introduction of different constraints on the object and on the PSF. In particular, we introduce a constraint on the PSF which is an upper bound derived from the Strehl ratio (SR), to be provided together with the input data. In this contribution we show the photometric error dependence on the crowding, having simulated images generated with synthetic PSFs available from the Phase-A study of the E-ELT MCAO system (MAORY) and different crowding conditions.

1 Introduction

Adaptive Optics (AO) has become a key technology for all the main existing telescopes (VLT, Keck, Gemini, Subaru, LBT) and is considered a kind of enabling technology for future giant telescopes as the European Extremely Large Telescope (E-ELT) [1] . To obtain high-precision quantitative information and improve the scientific exploitation of AO data, several efforts in a robust Point Spread Function (PSF) extraction method in a code for image analysis are needed.

Several photometric packages are available and commonly used by the scientific community: Romafot [2], DAOPHOT [3], DoPHOT [4], HSTPhot [5], Sextractor [6]. While they provided excellent results in the analysis of both ground based and HST data, none of them is specifically designed for AO systems: some of them rely on simple analytic PSF models that are not suited to AO. The first attempt to solve the problem of obtaining accurate photometry and astrometry from small field AO images has been made with the StarFinder code [7]. This code employs a constant and highly structured PSF which is calculated numerically from the brightest stars in the science field. We present in this paper the photometric analysis of an interesting science case using the blind deconvolution as a method for the reconstruction of the PSF. The extracted PSF and the background frame are supplied to StarFinder for the photometric and astrometric analysis.

We tested the blind deconvolution method in extreme conditions of crowding and Signal-to-Noise Ratio (SNR), measuring the photometric accuracy in two locations within a Giant Elliptical Galaxy in the Virgo Cluster (distance $\approx$ 18 Mpc), that represents an interesting and challenging science case [8] for the future high angular resolution camera MICADO@E-ELT [9], coupled with the Multi Conjugate Adaptive Optics module MAORY [10].

The images have been simulated using the MAORY PSFs in J and K_s bands available in the website (`http://www.bo.astro.it/maory/Maory/Welcome.html`). These PSFs have been computed by

[a] laura.schreiber@oabo.inaf.it
[b] andrea.lacamera@unige.it
[c] marco.prato@unimore.it

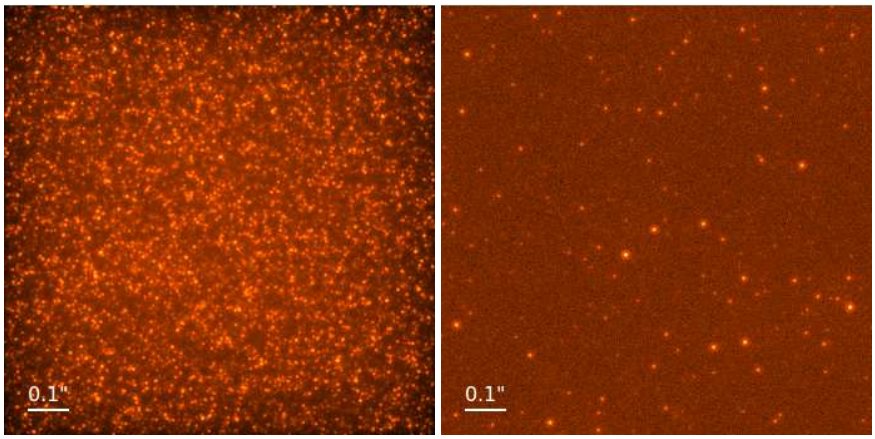

Fig. 1. Simulated images of a $1'' \times 1''$ stellar field in J band with two different crowding conditions. *(Left)*: extremely high crowding condition ($\approx$ 126000 stars/$arcsec^2$). *(Right)*: low crowding condition ($\approx$ 1000 stars/$arcsec^2$). These levels of crowding are typical at 0.1 and 2 effective radii respectively of an Elliptical galaxy in Virgo Cluster. The total integration time = 2 hours. The simulated images include stars with $24 \leq Ks \leq 31$ and $25.3 \leq J \leq 31.7$.

the MAORY consortium evaluating the MCAO performance during the phase A of the instrument. The MAORY PSF (zoomed J band central part in Figure 3, first panel) presents a really complicated shape, where the central component has the typical shape of the Airy disk, and the secondary structures can be attributed to the MCAO system properties, like the constellation of the 6 Laser Guide Stars (the secondary peaks arranged in the hexagonal configuration), and the residual light due to the non-perfect correction of the turbulence (external halo).

2 Simulated Data

With the exquisite resolving power of an ELT working at diffraction limit, thanks to Multi Conjugate Adaptive Optics capabilities, it will be possible to study down to the inner and crowded regions of galaxies beyond the Centaurus group, and in particular in the Virgo Cluster. In order to perform high precision astrometry and photometry exploiting the full potential of Adaptive Optics technique, the PSF extraction algorithm robustness and reliability are really important aspects that need to be taken into account.

In order to evaluate the effect of crowding and low SNR on the blind deconvolution PSF reconstruction, we simulated two stellar fields with levels of crowding typical at 0.1 and 2 effective radii respectively of an Elliptical galaxy in Virgo Cluster [8]. The available PSFs were computed for a reference "median seeing" atmospheric condition (seeing FWHM = $0.8''$ at 0.5μm wavelength and at zenith pointing) and for a "good seeing" condition (seeing FWHM = $0.6''$). We assumed the "good seeing" PSFs computed in the center of the MICADO FoV at the wavelengths Ks and J. Since the variation across the whole MICADO FoV is very low, we assumed a fixed PSF for each simulated frame.

For the considered science case, the input stellar lists, used to generate the frames, contain $\approx$ 126000/$arcsec^2$ stars brighter than $Ks = 31$ in the most crowded case, and $\approx$ 1000/$arcsec^2$ in the other case. Synthetic frames are generated from these lists in the corresponding bands, positioning the properly re-sampled MAORY PSF in the stars coordinates, scaling it to the correct flux considering 2 hours exposure time, adding the background due to the sky and the photon and the Read Out Noise (properly scaled for the number of exposures).

3 The blind deconvolution method

A classical way to restore the stellar object and the PSF is the minimization of a cost function depending on the statistical properties of the noise affecting the data. As concerns the RON, it is a realization of a Gaussian additive random variable with a known variance σ^2. According to [11], it can be approximated by a Poisson process with mean and variance being the same as σ^2 if the constant term σ^2 is added to the observed image **g**. If we add σ^2 also to the background **b**, then we can assume that the noise on **g** is purely Poissonian, thus leading to the minimization of the so-called Kullback-Leibler (KL) divergence (also known as Csiszár I-divergence [12]).

In order to improve the PSF reconstruction (necessary for an accurate detection in a crowded field) we use a novel method of blind deconvolution [13] based on an inexact alternating minimization method applied to the minimization of the KL divergence. The implemented algorithm is iterative and each iteration k consists of alternating an update of the object $\mathbf{f}^{(k)}$ and the PSF $\mathbf{h}^{(k)}$ by means of fixed numbers of iterations of the scaled gradient projection (SGP) method [14]. A scheme of the blind deconvolution is shown in Figure 2.

Among all the alternating minimization schemes proposed in the literature for blind deconvolution problems, the one we adopted has several advantages that makes it suitable for our application. First of all, it is a convergent scheme, in the sense that any limit point of the sequence $(\mathbf{f}^{(k)}, \mathbf{h}^{(k)})$ generated by the algorithm is a stationary point for the minimization problem [15]. Second, the alternating strategy allows to consider different constraints for each inner sub-problem. In our case, we can impose non-negativity on the image and an upper bound (based on the Strehl ratio value, supposed known) plus a normalization on the PSF. Third, the use of SGP allows an inexact minimization of each sub-problem, since the only requirement for the scheme to converge is the presence of an arbitrary upper bound on the inner iterations. Finally, the huge amounts of tests made on SGP in several applications (e.g., [16–18]) has led to an optimization of all the parameters defining the method, which allows the user to have at his disposal a fast and robust approach without the need for any problem-dependent parameter tuning.

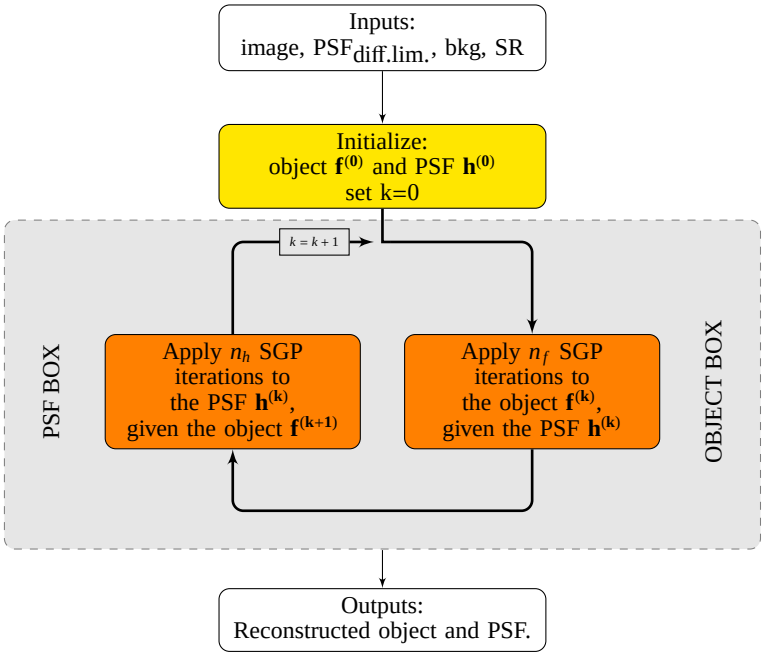

Fig. 2. Graphical representation of the alternating minimization scheme.

4 Results

We applied the blind deconvolution method described in the previous section to the input images. The initial guess of the algorithm is the auto-correlation of the diffraction limited instrument PSF, which satisfies the SR constraint. We chose a fixed pair ($n_f = 50, n_h = 2$) for the inner iterations (see Figure 2) and a variable number of outer iterations (that depends on the input image).

We tested the reconstructed PSFs by performing the photometric analysis on the input images using the StarFinder code. The package itself is able to estimate the background and extract a numerical PSF template from the frame, but it can also accomplish the analysis using a PSF and a background frame supplied by the user.

We checked the performance of the blind algorithm in two different cases: when the background is perfectly known and when it has been estimated from the data. In the latter case, the PSF estimation requires two steps: (1) a first background estimation and an extraction of the PSF; (2) after a preliminary photometric analysis, most of the stars can be subtracted and the background refined by smoothing the residual image. The new background frame can be used for the final PSF estimation.

4.1 Analysis of the reconstructed PSFs

In the case of background estimated from the data, we first reconstructed the preliminary PSF starting from the estimated background frame with a median value of 37841.0 counts (the background added to the input images is a constant value equal to 37661 counts). Two different numbers of outer iterations have been chosen, namely 200 and 500 iterations, giving an "early stopped" and a "late stopped" reconstruction, respectively.

By using these PSFs, two different backgrounds have been estimated from the input image. In the first case (early stop background) the frame has a median value of 37812.4 counts. In the second case (late stop background) we have a similar value: 37821.6 counts. Both values are slightly close to the true value with respect to the preliminary value.

According to the previous description, we completed the estimation of the PSF with the second step. Again, after 200 and 500 iterations we obtained the final "early stopped" PSF and the "late stopped" PSF, respectively. The true PSF, the initial PSF of the blind algorithm, the two final (blind) PSFs, and the numerical (StarFinder) PSF are shown in Figure 3.

Moreover, an horizontal cut of the central core of the five PSFs shown in Figure 3 is given in Figure 4.

4.2 Photometric analysis

We show a comparison among the analysis accomplished by using different PSFs and making different hypothesis on the image background knowledge. The photometric accuracy for each case has been evaluated matching the input star list with the catalogue of stars found and measured by StarFinder assuming different PSFs. The considered PSFs are: the true one, used as input for the frames generation, the one extracted by the frame using the blind deconvolution method, and the numerical PSF extracted by the frame using the StarFinder specific package. For what concern the background, we considered again the true one, the mean value of which is perfectly know from the image simulation input data, and an iteratively estimated one. The results using different PSFs have been compared in the same background knowledge conditions, being the estimation of the PSF and of the background closely related to each other, especially in presence of very extended PSF halos. We studied the PSF quality through completeness of the detections and photometric error analysis, that represent the two most important effects that dominate the ability to carry out an accurate scientific analysis of deep images of resolved stellar populations. The errors from photometry determine how accurately we are able to estimate the PSF and the completeness, i.e. the fraction of detected stars of a given magnitude, determines the achievable star catalogue depth, closely related to the background estimation capability.

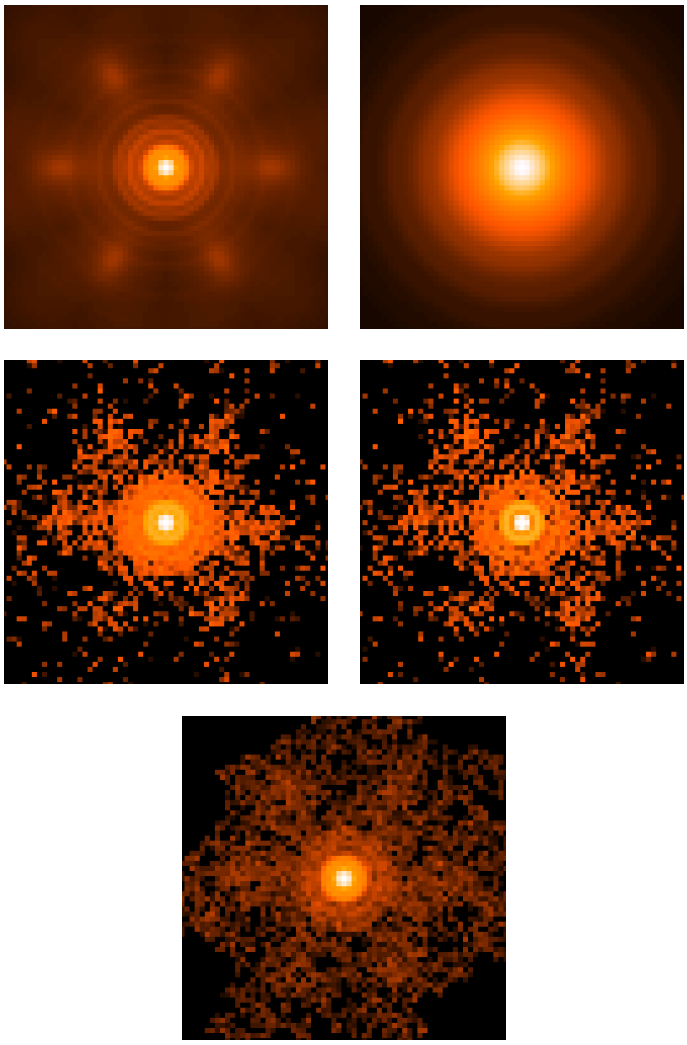

Fig. 3. *(From left to right and from top to bottom)*: the true PSF, the initial PSF ($\mathbf{h}^{(0)}$) of the blind algorithm, the blind PSF after 200 iterations, the blind PSF after 500 iterations, and the numerical PSF (computed by StarFinder) in the case of background estimated from the data.

Figure 5 shows the comparison between the analysis carried out using the true PSF and the PSF extracted with blind deconvolution method supposing to know the true background for both the PSF estimation and the photometric analysis. The completeness and the photometric errors are comparable.

Figure 6 shows the same analysis considering a background estimated from the data frame and four different PSFs: the StarFinder numerical PSF, the “early stopped” and “late stopped” blind PSFs (see previous section) and the true PSF (using however the true background) for comparison with Figure 5. The plots point out that the numerical PSF and the “early stopped” blind PSF give similar results, while the “late stopped” blind PSF shows an higher photometric error at the brightest magnitudes due to the error in modelling the PSF core, that contains the majority of the signal. This difference between the two blind PSFs is not visible in the completeness plot, because completeness depends strongly on the background estimation goodness, as demonstrated by the comparison with the black curves related to the true PSF and true background case.

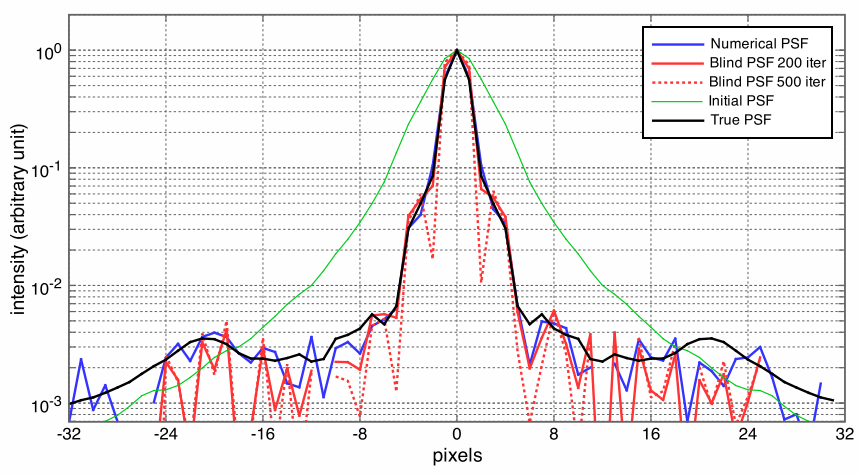

Fig. 4. The horizontal cuts of the numerical PSF (blue line), of the reconstructed PSFs (after 200 iterations solid red line and after 500 iterations dotted red line), of the initial PSF (green line), and of the true PSF (black line).

5 Conclusions

In this paper we presented the photometric accuracy and completeness obtained using the blind deconvolution method for the extraction of the PSF from simulated data. The frames have been simulated using the predicted PSF of MAORY, the future MCAO module of the E-ELT telescope, assuming the "good seeing" J and K_S PSFs available on the MAORY consortium official website. The considered science case, two stellar fields with levels of crowding typical at 0.1 and 2 effective radii respectively of an Elliptical galaxy in Virgo Cluster, represents an "extreme" case in terms of crowding conditions and low SNR and therefore it is an interesting testbench for the blind deconvolution algorithm. We conclude that:

- the blind deconvolution is a valid and robust algorithm for the PSF reconstruction even in extremely crowded fields and in condition of low SNR;
- the blind reconstructed PSF is independent of the selection of the stars, while the numerical PSF carried out by StarFinder is not;
- the estimation of the background is a crucial issue in both numerical and blind approach. An error in the background estimation strongly affects the limiting magnitude detectable. This is an important aspect when AO images of crowded fields are involved because of the strong contribution of the PSF extended halo to the background;
- the photometric error obtained using blind PSF gets higher when the number of iterations for the PSF extraction is not well tuned. In particular, an excessive number of iterations affects the modeling of the PSF core that contains the majority of the signal, producing an higher photometric error in the brightest stars magnitude estimation. This parameter (number of iterations) has to be tuned carefully;
- when the number of iterations for the blind PSF estimation is well tuned, the performance of the algorithm is comparable with other PSF extraction algorithms (i.e. numerical PSF) in spite of the extremely unfavorable conditions (low SNR and high crowding).

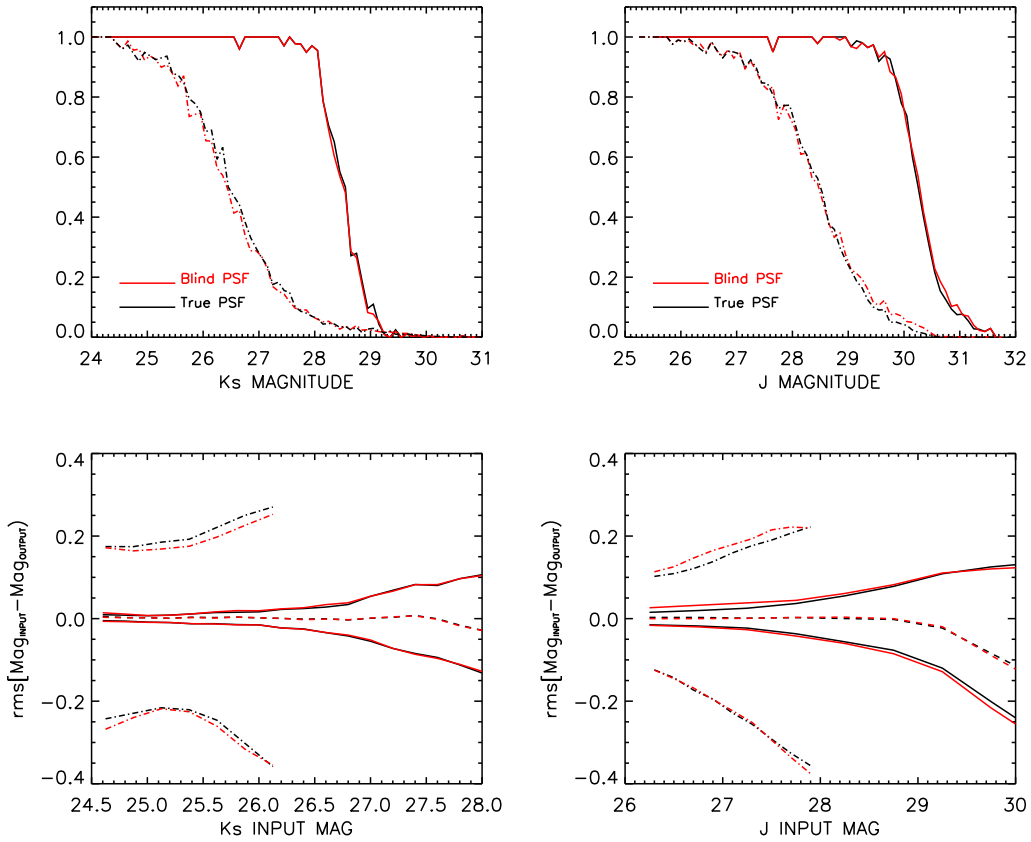

Fig. 5. *(Upper panels)*: Completeness plots in K_s *(left)* and J *(right)* bands for the two considered crowding conditions and using the true PSF (black lines) and the blind deconvolution PSF (red lines) for the data analysis (2 σ detection threshold). The background for both the blind PSF extraction and the data reduction has been considered as perfectly known. In each plot the extremely crowded case (dotted-dashed lines) and the less crowded case (solid lines) are over-plotted. *(Lower panels)*: matching the catalogue of the frame input stars and the result of the data reduction, we computed the photometric error in K_s *(left)* and J *(right)* bands as a function of the input magnitudes. The asymmetrical distribution of the photometric errors is due to blending effects.

6 Acknowledgments

This work has been partly supported by Istituto Nazionale di Astrofisica by the grant TECNO INAF 2010 “Exploiting the adaptive power: a dedicated free software to optimize and maximize the scientific output of images from present and future adaptive optics facilities”. L.S. acknowledge the support of INAF through the 2011 postdoctoral fellowship grant. L.S. wants to thank Laura Greggio and Renato Falomo (INAF - Astronomical observatory of Padova) for their essential suggestions and support in the simulated frames generation. M.P. is partially supported by a grant of the Italian GNCS - INdAM (Gruppo Nazionale per il Calcolo Scientifico - Istituto Nazionale di Alta Matematica).

References

1. Gilmozzi, R. et al., Proc SPIE **7012**, (2008) 701219.
2. Buonanno, R. et al., A&A **126**, (1983) 278.

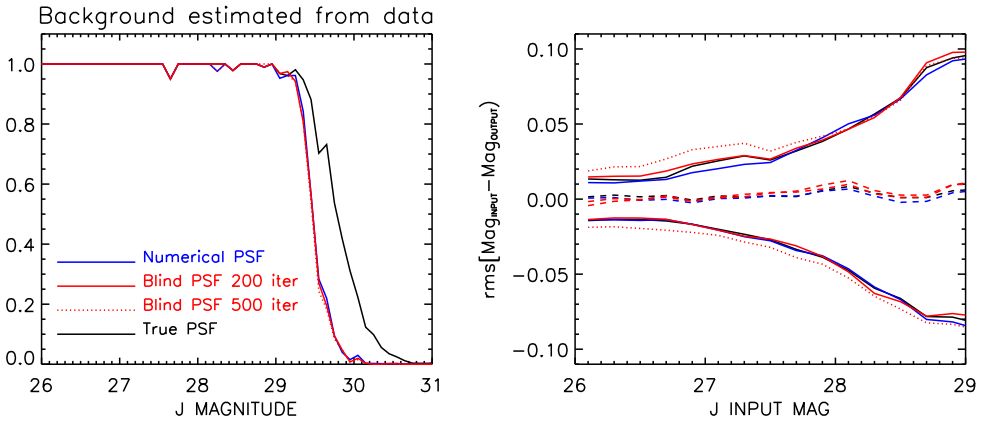

Fig. 6. *(Left)*: Completeness plot in *J* band in low crowding condition using the "early stopped" blind PSF (solid red lines), the "late stopped" blind PSF (dotted red lines) and the numerical PSF (blue lines) extracted by StarFinder. The σ detection threshold is fixed at 3 for all the cases considered. The background has been estimated from the data. For comparison, also the completeness obtained by using both the true PSF and background is over-plotted in black. *(Right)*: Photometric error in *J* band in low crowding condition by using again the same PSFs and background.

3. Stetston, P. B., PASP **99**, (1987) 191.
4. Schechter, P. L. et al, PASP **105**, (1993) 1342.
5. Dolphin, A. E., PASP **112**, (2000) 1383.
6. Bertin, E. & Arnouts, S., A&AS **117**, (1996) 393.
7. Diolaiti, E. et al., A&AS **147**, (2000) 335.
8. Greggio, L. et al., PASP **124**, (2012) 653.
9. Davies, R. et al., Proc SPIE **7735**, (2010) 77352A.
10. Diolaiti, E. et al., This symposium, (2013).
11. Snyder, D., in The restoration of HST images and spectra, ed. R. L. White, & R. J. Allen, Space telescope Science Institute, (1990) 56.
12. Csiszár, I., Ann. Stat. **19**, (1991) 2032.
13. Prato, M. et al., Inverse Prob., **29**, (2013) 065017.
14. Bonettini, S. et al., Inverse Probl. **25**, (2009) 015502.
15. Bonettini, S., IMA J. Numer. Anal. **31**, (2011) 1431.
16. Benvenuto, F. et al., Inverse Probl. **26**, (2010) 025004
17. Prato, M. et al., A&A **539**, (2012) A133.
18. Zanella, R. et al., Inverse Probl. **25**, (2009) 045010.